A differential frost heave model: cryoturbation-vegetation interactions

R.A. Peterson, D.A. Walker, V.E. Romanovsky, J.A. Knudson, M.K. Raynolds
University of Alaska Fairbanks, USA

W.B. Krantz
University of Cincinnati, USA

ABSTRACT: We used field observations of frost-boil distribution, soils, and vegetation to attempt to validate the predictions of a Differential Frost Heave (DFH) model along the temperature gradient in northern Alaska. The model successfully predicts order of magnitude heave and spacing of frost boils, and can account for the circular motion of soils within frost boils. Modification of the model is needed to account for the observed variation in frost boil systems along the climate gradient that appear to be the result of complex interactions between frost heave and vegetation.

1 INTRODUCTION

This paper discusses a model for the development of frost boils due to differential frost heave. The interactions between the physical processes of frost heave and vegetation characteristics are explored as a possible controlling mechanism for the occurrence of frost boils on the Alaskan Arctic Slope.

Frost boils are a type of nonsorted circle, "a patterned ground form that is equidimensional in several directions, with a dominantly circular outline which lacks a border of stones…" (van Everdingen 1998). Frost boils, also known as frost scars, mud boils and mud circles, consist of bare soil patches with diameter of 1–3 m. Frost boils are prevalent in the northernmost coastal regions underlain by continuous permafrost.

Frost heave is an uplifting of the ground surface due to ice lens formation within the active layer. Areas with frost boils typically heave significantly. *Differential frost heave*, laterally non-uniform frost heave, is believed to be a major contributor to the formation of frost boils (Hallet *et al*., 1988; Krantz 1990; Kessler *et al*., 2001). Differential frost heave (DFH) can also occur spontaneously during one-dimensional heaving (Peterson & Krantz 2003). This phenomenon is due to a physical instability in the one-dimensional frost-heave process, analogous to the formation of icicles due to the density-difference instability of water suspended above air. Patterns form when unstable one-dimensional processes evolve into multi-dimensional processes. In the case of DFH, these patterns can take the form of a three-dimensional network of frost boils. Once the three-dimensional pattern is initiated, subsequent processes such as non-uniform water transport and soil creep cause further differentiation. Ultimately, "spotted-tundra" landscapes develop, resulting in stable, three-dimensional systems, wherein the self-organizing process of frost-boil development is balanced by degrading geological processes such as soil creep. Washburn listed 19 possible mechanisms responsible for the formation of patterned ground (Washburn 1956). The model presented here explains the formation of patterned ground by differential frost heave. DFH is also responsible, at least in part, for the formation of sorted stone circles in Spitsbergen (Hallet *et al*., 1988). A recent model due to Kessler *et al*. (2001) for the genesis and maintenance of stone circles integrates DFH with soil consolidation, creep, and illuviation.

The study area is the Sagavanirktok River region in Northern Alaska. Loess is the parent material over most of this area. The Dalton Highway provides ready access to five study sites: West Dock, Deadhorse, Franklin Bluffs, Sagwon MNT and Sagwon MAT. A steep summer climate gradient exists in the area (14°C–28°C). Average mean July temperature (MJT) at the coast (West Dock) is about 6°C, while MJT for the furthest inland site (Sagwon) is about 13°C. Frost boils are locally distributed and cover 0–30% of the ground depending on the location. Small-scale topographic features such as slopes can cause marked changes in the abundance of frost boils, while uniform expanses can exist on the scale of 1000's of meters. One particularly interesting area is along the boundary between acidic and nonacidic tundra at the northern edge of the Arctic Foothills. Frost boils are prevalent north of the boundary and almost completely absent to the south. Also notable is a marked difference in vegetation on either side of this boundary (Walker *et al*., 1998). High water contents and silty soils combine to make ideal conditions for frost heave north of the boundary. To the south of the boundary lies moist acidic tundra (MAT), which includes dwarf-shrubs and tussock sedges. North of the boundary lies moist nonacidic tundra (MNT), which is characterized by graminoids. An abundance of frost boils exists north of the boundary while few are found to the south.

2 METHODS

A 10 × 10-meter grid was established at each of the five study sites in order to characterize the vegetation, frost-boil distribution and seasonal snow depth. Maximum thaw depth of the active layer was measured manually using a 1-meter metal probe. Measurements were made every half-meter in the 10 × 10-meter grids at all five study sites. Instrumentation was installed at each site to permit continuous, automatic data-logging of air temperature, active layer thickness, soil moisture, and permafrost temperatures. A custom-built apparatus for measuring differential frost heave was installed at each of the study sites. Two-meter metal support poles were anchored into the permafrost and a crossbar attached between them. Lightweight carbon fiber rods with plastic feet were placed through holes in the crossbar and allowed to move up and down freely. The feet of the rods were buried approximately 1-cm into the frost boil or inter-boil region. Net upward movement of the ground surface due to frost heave was measured manually by recording the location of the carbon fiber rod before and after ground freezing. Downward movement due to thaw subsidence was measured analogously. Characterization of the five selected sites was carried out during the summer field seasons of 2000 and 2001. Active layer depth, frost-boil abundance and distribution, and surface vegetation characteristics were recorded. Several frost-boils were excavated to examine the morphology. Characterization of the vegetation included abundance, plant type and distribution.

3 OBSERVATIONS

Several frost boils were excavated and examined at Franklin Bluffs. The top of the active layer began at the base of the vegetation and included only the thawed organic layer (when present) and underlying thawed mineral soil. The active layer was significantly deeper beneath the frost boils, up to 1.5 times the inter-boil depths. Although the frost boils typically had a surface relief up to 10 centimeters, the increased thaw depth beneath the boils was significant enough that there was a concave bowl-shape in the permafrost table beneath each frost boil. The deeper active layer beneath the frost boil and signs of frost action within the seasonally-thawed soil were evident. The entire active layer beneath the center of the boil was mineral soil, while the inter-boil regions typically had an organic layer on the order of 10 centimeters overlying mineral soil. Disturbed soil horizons was evident in the cross section beneath the center of the boil in what appears to be the result of upward soil movement from the base of the active layer. A strong horizontal platey structure was evident both within and between the boils. However, a greater number and closer spacing of these horizontal regions indicated increased ice lensing beneath the frost-boil centers.

Frost boils were absent at both West Dock, uncommon at Sagwon MAT, and most prevalent at Deadhorse and at Franklin Bluffs. The relatively few frost boils observed at Sagwon MAT were approximately 50% smaller in diameter than those at Deadhorse and Franklin Bluffs. Close examination at Sagwon MAT revealed what appeared to be several relic frost boils that had become overgrown with moss and shrubs. This observation indicates that vegetation succession caused the mechanisms that drive frost boil development and maintenance to be effectively "turned off". At the southern end of the climatic gradient (Sagwon), more extensive moss cover and tall plant canopies insulated the soil surface causing a decrease in the seasonal thaw depth. Although the Sagwon MNT and MAT sites were very close in proximity (within 1 km) and thus were exposed to similar summer temperatures, the MAT site had a significantly shallower active layer. The conspicuous absence of frost boils and significantly different vegetation accounted for this marked difference in active layer. Furthermore, the MAT site had a deeper organic layer that acted as an insulator during the warm summer months. The shallow active layer at West Dock was due to its colder climate and absence of frost boils. The absence of frost boils here was caused mainly by thick organic soil horizons and gravelly parent material within 30 cm of the surface. The summer warming index (SWI) had a monotonically increasing trend with distance from the coast while the active layer thickness was a function of both of air temperature and vegetation cover.

The distribution of ground-surface heave in 2001 for sites with evidence of frost-boil activity is shown in Figure 1. The two sites at Deadhorse displayed the greatest degree of differential heave with almost a
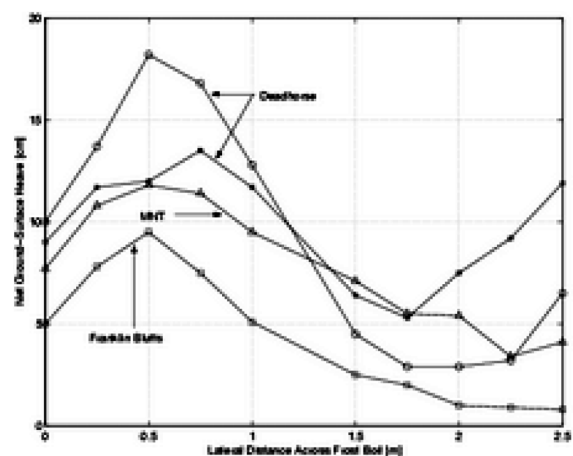

Figure 1. Net ground-surface heave recorded in spring from the heave meters. Errors in the measurements are ±1 mm.

5-fold difference in heave between the center of the frost boil and the inter-boil region. The greatest heave recorded was 18 cm at one Deadhorse site.

4 DIFFERENTIAL FROST HEAVE MODEL

The model for differential frost heave is based on the one-dimensional numeric frost heave model of O'Neill and Miller (1985). Fowler (1987) and Fowler and Krantz (1994) later extended the model to multiple dimensions by properly incorporating regelation, and arrived at an analytic solution to the one-dimensional problem by the judicious use of scaling arguments. A complete mathematical description of the DFH model is in Peterson (1999).

The model is based on the schematic of a soil cross-section undergoing top-down freezing shown in Figure 2. The freezing soil is divided into three regions: (1) the upper, frozen soil where relatively little liquid water is present and extensive ice lensing occurs, (2) the three-phase (liquid water, ice and soil) frozen fringe within which most all freezing occurs, and (3) the lower, unfrozen, saturated soil where no ice is present. The combined three regions make up the active layer. It is assumed that negligible solutes are present in any of these regions. The bottom boundary of the third region, z_b is the impermeable permafrost boundary at the constant prevailing freezing temperature. In this analysis, the effect of up-freezing is neglected and the permafrost boundary is assumed stationary.

The resulting model is a pair of coupled, vector equations that describe the velocities of both the freezing front and ice at the location of the lowest ice lens.

$$\mathbf{V_f} = f_1(S, W_l, E)\,\mathbf{G_i} + f_2(S, W_l, E)\,\mathbf{G_f} \qquad (1)$$

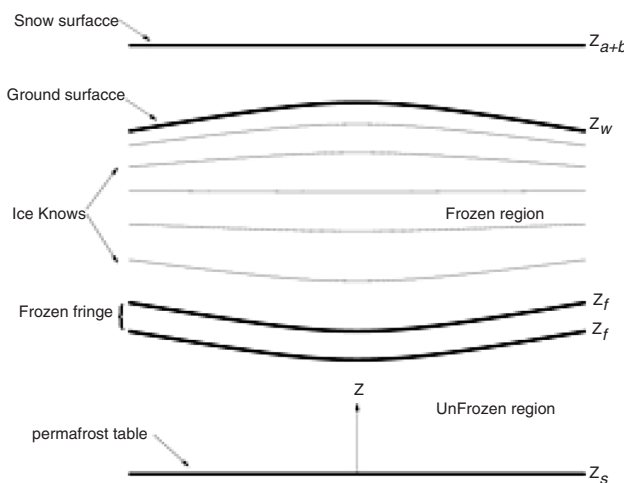$$\mathbf{V_i} = g_1(S, W_l, E)\,\mathbf{G_i} + g_2(S, W_l, E)\,\mathbf{G_f} \qquad (2)$$

Figure 2. Schematic of soil undergoing top-down freezing on which the DFH model is based. Ice lenses exist in the frozen region and permafrost underlies the active layer.

In the above equations, S is a set of parameters describing the soil (e.g. density, porosity), E is a set of parameters describing the environmental conditions (e.g. current depth of freezing, surface load), W_l is the unfrozen water content by volume, and $f_{1,2}$ and $g_{1,2}$ are complicated functions of these parameters (see Fowler and Krantz, 1994, for the exact form). The freezing front velocity is $\mathbf{V_f}$, the ice velocity is $\mathbf{V_i}$, and the temperature gradient at z_l is $\mathbf{G_i}$ in the unfrozen region and $\mathbf{G_f}$ in the frozen region. Bold font indicates vector quantities.

The intent of this analysis is to investigate the spontaneous emergence of a multidimensional, patterned solution from a one-dimensional solution. First, a linear stability analysis (LSA) is performed to determine the parameter space in which the model is linearly unstable. Next, the multi-dimensional frost-heave model is solved numerically. Due to expected radial symmetry on flat ground, the numerically arduous problem was solved in two dimensions, while the three-dimensional analog will be qualitatively similar.

The time-evolution problem requires a rheological description of the frozen soil. The time-scale for relaxation of frozen soil under under small strain is hours (Tsytovich, 1975). A purely viscous rheology is most applicable in this case due to the relatively fast relaxation times for frozen soils. Similar to models for glacier flow (Paterson, 1994), a thin-film approximation is used. The x- and z-momentum equations for a newtonian fluid are simplified using scaling arguments. The inertial terms in both equations are negligible, as is the viscous term for z momentum. The boundary conditions are: (1) hydrostatic pressure at z_f, (2) prescribed velocity at z_f obtained from the frost-heave equations, and (3) zero tension at the free surface, z_s. By introducing newtonian viscous flow equations, a viscosity of the frozen soil is required. A characteristic viscosity for frozen soil is 10^{14} Pa s (Sayles, 1988) based on creep experiments.

Although minimal viscous relaxation occurs during the freezing process due to the high viscosity of frozen soil, significant creep may occur during periods of thaw. The above model may be applied during periods of thawing by setting the ice velocity $\mathbf{V_i}$ to zero and adjusting the soil viscosity to a value appropriate for thawed soil. The thawed-soil viscosity can be a strong function of degree of saturation. For simplicity, a constant value of 10^{11} Pa s is assumed.

5 MODEL PREDICTIONS

The conditions resulting in linear instability identified by the LSA may be used as initial conditions in the time-evolution DFH model. The initial ground-surface perturbation is a periodic wave with a 1.0-cm initial
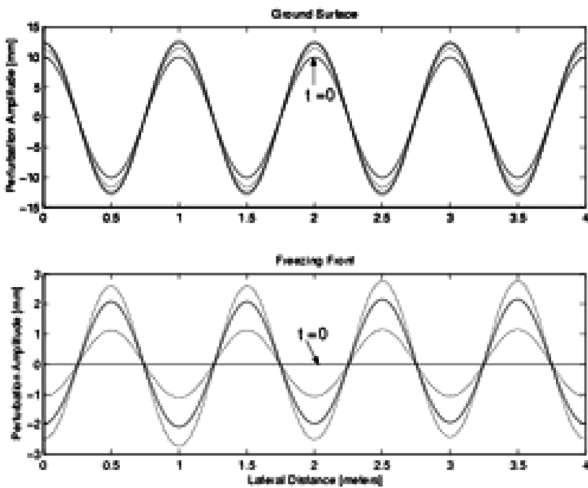
Figure 3. Time series showing the perturbation amplitudes for both the ground surface and freezing fronts. Amplitudes increase with time and each curve is for $\Delta t = 7.3$ days. The freezing front is initially flat and the ground surface amplitude is initially 1 cm. Amplitudes are measured relative to their mean location, so the above figure does not show the increase in freezing depth that is occurring.
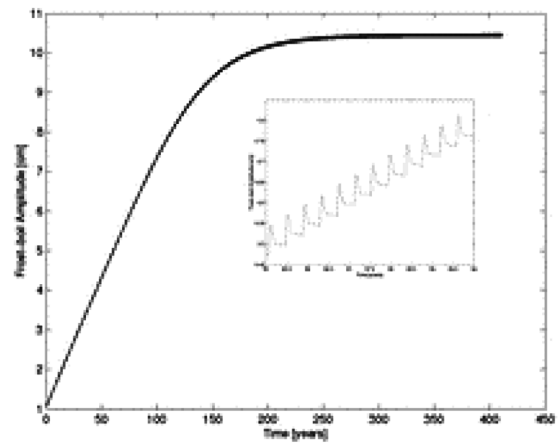

Figure 4. Frost-boil amplitude during growth and eventual stabilization due to DFH in the winter and soil creep in the summer. At approximately 100 years, increasing rate of soil creep balance the decreasing rate of DFH.

amplitude. The freezing front is initially flat. The initial *average* depth of freezing is 5.0 cm. The perturbation amplitudes are measured as the difference between the wave peak and the mean vertical location of the surface. The average depth of freezing increases with time. Since the perturbation amplitudes are measured from the mean vertical location of the surface, they may increase or decrease.

Figure 3 shows a time series of perturbation amplitudes of the ground surface and freezing front for a Deadhorse soil under 25 cm of snow and an air temperature of $-10°C$. The wavelength of the initial ground-surface perturbation is 1 meter, which is typical of frost-boil diameters observed in the field. Successive curves represent $\Delta t = 7.3$ days, and the entire series is about one month. The amplitudes of both surfaces grow with time for the series shown here. Furthermore, the perturbations are 180° out-of-phase. An initial finite depth of freezing is required since the DFH model has a singularity when freezing first initiates (i.e. $z_s = z_f$). The initial 5-cm depth of freezing is a typical magnitude of non-heaving surface organic layers (Romanovsky and Osterkamp, 2000).

Freezing simulations were performed to freezing depths of 50 cm – typical active layer depths in the Deadhorse region. The ground surface perturbation begins to decrease in amplitude after reaching a freezing depth of about 28 cm. The freezing front perturbation also begins to decrease in magnitude after a freezing depth of 34 cm is reached. This behavior indicates a weakening in the mechanism driving differential frost heave at larger depths of freezing. As the depth of freezing increases, a smaller range of

wave numbers (corresponding to the smallest wavelengths) are linearly unstable. The driving force for differential frost heave is lateral heat transfer through the corrugated ground surface (Peterson and Krantz, 2003). As the depth of freezing increases, the benefits of lateral heat transfer are overcome by the stabilizing forces of elasticity (in the LSA model) and viscous relaxation (in the time-evolution model).

These simulation results indicate that finite-amplitude, two-dimensional perturbations in the ground surface and freezing front will increase in magnitude from an initially small perturbation in the ground surface. Although both perturbations begin to decrease in amplitude at deeper depths of freezing, a net increase in magnitude is realized for active layer depths typical of the Alaskan Arctic Coastal Plain.

After a single freezing season, the ground-surface perturbation amplitude increases approximately 18%. An order-of-magnitude estimate for the number of years, n, required for a 1-mm initial perturbation to evolve into a 20-cm high frost boil is

$$\ln(\eta_{final}/\eta_{inital}) = n \ln(\eta_{t+1}/\eta_t) \qquad (3)$$

and therefore,

$$n = \ln(200/1)/\ln(1.18) = 32 \text{ years} \qquad (4)$$

This prediction of pronounced pattern development in 32 years is lower than other reported predictions that are on the order of hundreds of years (Mackay, 1980). However, this estimate does not account for degrading effects, such as soil creep during summer thaw.

A model that can estimate the time required for pattern development due to DFH in spite of the degrading effects of soil creep can now be constructed. The DFH model is run for several freezing seasons and combined with the viscous-relaxation (soil creep) model during the summer months. The results of this simulation are shown in Figure 4 where the ground-surface

perturbation amplitude is plotted as a function of time in years. The saw-tooth shape reflects the growth due to DFH followed by yearly subsidence due to viscous relaxation. After approximately 100 years, the pattern amplitude begins to stabilize with a height of approximately 15 centimeters. This equilibrium occurs because the growth due to DFH eventually balances the degradation due to viscous relaxation after a critical amplitude is reached. The equilibrium amplitude is a function of several physical properties measurable in the field or laboratory. Decreasing the viscosity of the thawed soil results in smaller equilibrium amplitudes. The viscosity is a function of the soil type and degree of saturation among other things. Thus, different soil types may have patterns with different heights, which may explain the different height-to-width ratios observed globally.

The ability of the time-evolution model to quantitatively predict the amount of DFH observed in the field is limited without definitive physical property data for the soils, and without taking into account the effects of an evolving vegetation mat as frost-boil ecosystems develop. Thus, exact quantitative agreement is currently beyond the capability of the model. However, it is encouraging to see that the DFH model does predict order-of-magnitude height and wavelength observed in the field as well as the time scale for pattern development and equilibration.

6 CRYOTURBATION

Cryoturbation is soil movement due to frost action. Where surface patterns such as frost boils are present, evidence of a vertical circular motion is typically observed. Soil moves upward beneath frost boils and downward in the inter-boil regions as shown in Figure 5. Several theories have been proposed to explain this circular motion. Some of these include the analytic models for Rayleigh free convection (Gleason *et al.*, 1986; Krantz 1990) and buoyancy-induced circulation (Hallet and Waddington 1992), and probabilistic models based on differential frost heave (Kessler *et al.*, 2001). The underlying mechanism responsible for soil circulation remains a disputed issue.

The DFH model presented here analytically predicts a circular soil motion based on differential heaving during the winter and viscous relaxation during the summer. Figure 5 shows particle trajectories predicted by the model during the course of several hundred years of differential heaving and settling. Soil near the bottom of the active layer is moved upward and inward due to DFH. Conservation of mass and viscous relaxation causes a downward motion of soil in the inter-boil regions. Purely viscous relaxation during the summer is shown in Figure 6 where the arrows indicate
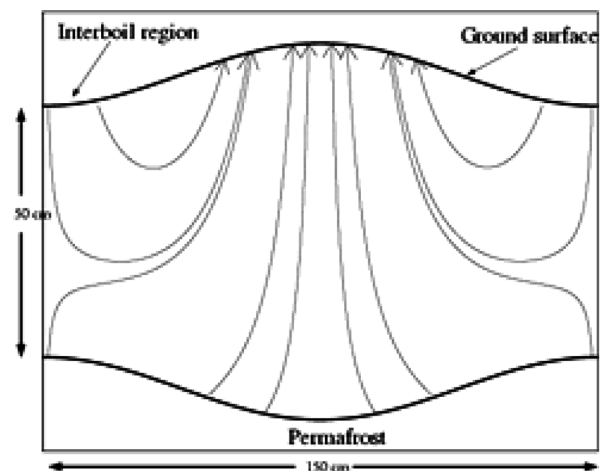

Figure 5. Particle trajectories over several hundred years of differential heaving and soil creep. Soil particles move downward in the inter-boil region and upward beneath the center of the frost boil.
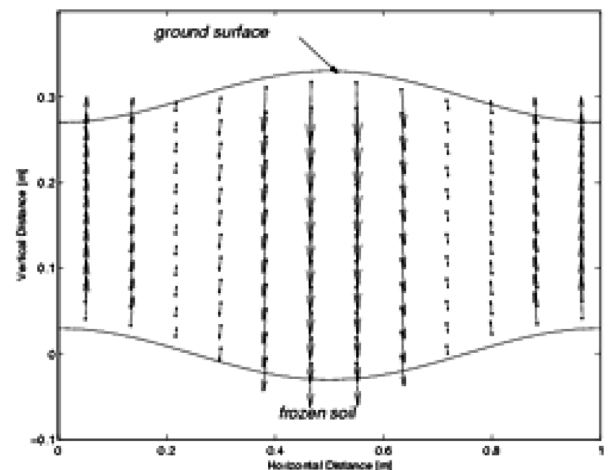

Figure 6. Particle trajectories of unfrozen soil using a viscous-relaxation model to describe soil creep. The arrows indicate direction and relative magnitude of soil particles.

relative speed and direction of the soil matrix. The tops of frost boils creep downward and conservation of mass causes the inter-boil regions to rise slightly.

The trajectories shown in Figure 5 are based only on DFH and viscous relaxation. Buoyancy-induced forces such as described by Hallet and Waddington (1992) may provide a concurrent mechanism for cryoturbation. Because "buoyancy seems incapable of driving wholesale soil circulation in a laterally uniform active layer" (Hallet and Waddington 1992), DFH likely plays a key role in the overall mechanism, as Hallet and Waddington assert. Coupling these two models to predict the net soil motion will be straight forward when conclusive values for viscosity of both thawed and frozen soils, as occur in the field, become available. Nonetheless, it is encouraging to see that the DFH model does predict the circular soil motion that appears to be occurring in many recurrently frozen soils.

7 CONCLUSIONS

Frost boil size and density do not correspond with the coastal climate gradient as might be expected. Instead, the vegetation cover appears to play a constraining effect on frost heave and frost-boil development. The relative absence of active frost boils in the MAT region may be the result of taller, more insulative plant communities, which mitigates frost-boil development. A time-evolution DFH model indicates that small, two-dimensional perturbations grow in time. The degrading effects of viscous relaxation by soil creep counter-balance the DFH mechanism. Ultimately a two-dimensional pattern stabilizes with amplitude on the order of 10 cm and a wavelength on the order of 1 meter. The model predictions for frost-boil size and occurrence agree reasonably well with observations made on the Alaskan Arctic Coastal Plain. Coupling DFH during the winter with soil creep in the summer results in a net circular soil motion that is upward beneath the frost boils and downward in the inter-boil regions. It is reasonable to believe that other mechanisms, such as buoyancy-induced circulation, may be acting in concert with the mechanisms described here. However, concurrent mechanisms are not necessarily required to explain the circular soil motion occurring during cryoturbation.

REFERENCES

Fowler, A.C. 1987. *Mathematical Models in the Applied Sciences*, Cambridge University Press, Cambridge, 402 pp.

Fowler, A.C. & Krantz, W.B. 1994. Generalized secondary frost heave model. *SIAM J. Appl. Math.* 54, 1650–1675.

Gleason, K.J., Krantz, W.B., Caine, N., George, J.H. & Gunn, R.D. 1986. Geometrical aspects of sorted patterned ground in recurrently frozen soils. *Science*, 232, 216–220.

Hallet, B., Prestrud, S.A., Stubbs, C.W. & Carrington, E.G. 1988. Surface soil displacement in sorted circles, western Spitsbergen. *Proceedings Fifth International Conference on Permafrost*, Trondheim, Norway, 770–775.

Hallet, B. & Waddington, E.C. 1992. Buoyancy forces induced by breeze-thaw in the active layer: implications for diapirism and soil circulation. *Periglacial Geomorphology*, Wiley, Chichester, 251–279.

Kessler, M.A., Murray, A.B., Werner, B.T. & Hallet, B. 2001. A model for sorted circles as self-organized patterns. *Journal of Geophysical Research*, 106, 13287–13306.

Krantz, W.B. 1990. Self-organization manifest as patterned ground in recurrently frozen soils. *Earth-Science Reviews* 29, 117–130.

Mackay, J.R. 1980. The origin of hummocks, western Arctic coast, Canada. *Candian Journal of Earth Sciences*, 17, 996–1006.

Paterson, W.S.B. 1994. *The Physics of Glaciers*, Pergamon, Oxford.

Peterson, R.A. 1999. *Differential Frost Heave Manifest as Patterned Ground-Modeling, Laboratory and Field Studies*. Ph.D. Thesis, Univ. Colorado, Boulder.

Peterson, R.A. & Krantz, W.B. 2003. A mechanism for differential frost heave and its implications for pattern-ground formation. *Journal of Glaciology,* submitted.

Ray, R.J., Krantz, W.B., Caine, T.N. & Gunn, R.D. 1983. A model for sorted patterned-ground regularity. *Journal of Glaciology*, 29, 317–337.

Romanovsky, V.E. & Osterkamp, T.E. 2000. Effects of unfrozen water on heat and mass transport processes in the active layer and permafrost. *Permafrost and Periglacial Processes*, 11: 219–239.

Sayles, F.H. 1988. State of the art: Mechanical properties of frozen soil. In *Fifth International Symposium on Ground Freezing*, Jones, R.H., Holden, J.T. (eds.) Brookfield, Rotterdam, 143–159.

Tarnocai, C. & Zoltai, S.C. 1978. Earth hummocks of the Canadian arctic and subarctic. *Arctic and Alpine Research*, 10, 581–594.

Tsytovich, N.A. 1975. *The Mechanics of Frozen Ground*, McGraw-Hill, Washington DC, 426 pp.

van Everdingen, R.O.E. 1998. *Multi-language Glossary of Permafrost and Related Ground-ice Terms*. University of Calgary: Calgary.

Walker, D.A., Auerbach, N.A., Bockheim, J.G., Chapin, F.S. III, Eugster, W., King, J.Y., McFadden, J.P., Michaelson, G.J., Nelson, F.E., Oechel, W.C., Ping, C.L., Reeburg, W.S., Regli, S., Shiklomanov, N.I. & Vourlitis, G.L. 1998. Energy and trace-gas fluxes across soil pH boundary in the Arctic, *Nature*, 394, 469–472.

Washburn, A.L. 1956. Classification of patterned ground and review of suggested origins. *Geological Society of America Bulletin* 67: 823–865.